coatings

MDPI

Article

Microstructure and Texture of Pure Copper under Large Compression Deformation and Different Annealing Times

Xiuqing Li [1,2,*], Qian Zhang [1], Wenpeng Lou [1], Fengjun Li [3], Jianjun Liang [4] and Shimin Gu [4]

[1] National Joint Engineering Research Center for Abrasion Control and Molding of Metal Materials, Henan University of Science & Technology, Luoyang 471003, China
[2] Henan International Joint Laboratory for High Temperature Refractory Metal Materials, Henan University of Science & Technology, Luoyang 471003, China
[3] First Tractor Company Limited, Luoyang 471004, China
[4] Nanyang North Hongyu Electromechanical Manufacturing Company Limited, Nanyang 474661, China
* Correspondence: xqli@haust.edu.cn

Abstract: In this study, the plastic deformation of pure copper under room-temperature compression and different annealing times was examined, and the microstructure and texture evolution were studied via scanning electron microscopy (SEM), electron backscatter diffraction (EBSD), and microhardness tests. The results showed that when the deformation degree was 93.75%, the microhardness increased from 76 HV (Vickers hardness) before deformation to 110 HV. After annealing, the hardness decreased with increasing annealing time, and the pure copper grain size could be refined from 150 μm to 6.15 μm. An increase in annealing time did not continue to promote recrystallization, while the effect on grain refinement was weakened. The geometrically necessary dislocation (GND) density decreased from $6.0 \times 10^{14}/m^2$ to $4.83 \times 10^{14}/m^2$ after annealing, which implies that static recrystallization occurs at the cost of dislocation consumption during the annealing process. The compression deformation of pure copper produced a strong deformation weave (<001> orientation), and a portion of the deformation weave within the material was transformed into a recrystallization weave (<111> orientation) after the annealing process.

Keywords: pure copper; room temperature compression; anneal; microstructure; texture

Citation: Li, X.; Zhang, Q.; Lou, W.; Li, F.; Liang, J.; Gu, S. Microstructure and Texture of Pure Copper under Large Compression Deformation and Different Annealing Times. *Coatings* **2023**, *13*, 2093. https://doi.org/10.3390/coatings13122093

Academic Editor: Csaba Balázsi

Received: 18 October 2023
Revised: 29 November 2023
Accepted: 14 December 2023
Published: 16 December 2023

1. Introduction

Pure copper has been widely used in the electrical, light, machinery manufacturing, construction, and national defense industries, among others, due to its good electrical and thermal conductivity, excellent corrosion resistance, and good ductility [1–4]. With the rapid development of modern industries, the requirements for material performance are growing. As a key material of the equipment manufacturing industry, the performance of pure copper determines its effectiveness in applications. Coarse-grained cast pure copper results in a lower performance. According to the Hall–Petch formula [5], the smaller the grain size of a metal material is, the better its mechanical properties are. In this context, researchers favored optimizing the performance of the majority of the materials by refining the grain size of the materials.

Plastic deformation methods include rolling, upsetting, forging, extrusion, and so on [6–9]. Pfetzing-Micklich et al. [10] introduced a new micro-shear experiment using a double-shear pure copper specimen, and evidence for localized shear was provided. Yannick et al. [11] found that pure nanocrystalline copper had near-perfect elastoplastic behavior, and this behavior was observed during tensile tests. A basis for plastic (and superplastic) formation was provided. Sakharov et al. [12] proposed a new model that describes primary recrystallization in pure copper, and the growth rate of recrystallization nuclei could be determined. An equation relating the volume fraction of the recrystallized pure copper material to the temperature and annealing time was derived. Konkova et al. [13]

studied grain structure development and texture evolution during/after the cryogenic rolling of pure copper. They found that microstructure evolution after cryogenic rolling was a complex process, and recrystallization probably occurred during static storage at room temperature. In a study by Song et al. [14], it was shown that the grain size of pure copper could be refined from 100 μm to 6.5 μm via cross-rolling, achieving a 90% thinning rate. Zhou et al. [15] processed a pure copper plate through one to six cycles of asynchronous cumulative stacking rolling deformation at room temperature. Due to the shear stress generated during the rolling deformation process, the grain size of pure copper was refined from about 30 μm to about 5 μm after rolling, and the performance was continuously optimized along with the process. It can be observed in the literature [16,17] that grain sizes can be refined to 3 μm in the first pass of multi-pass rolling at high temperatures, but grain sizes cannot be refined in the subsequent several passes [18].

These methods have the common advantage of being continuously repeatable experiments that can refine grain sizes until ultra-fine grains are produced [19–22]. In the original organization, there were a large number of small-angle grain boundaries. During the deformation and annealing process, many sub-grain boundaries form within this organization. Adjacent sub-grain boundaries on dislocations disappear through climbing and slipping, resulting in the merging of sub-crystals, thus transforming small-angle grain boundaries into large-angle grain boundaries and thereby achieving the goal of grain refinement. Although these deformation methods can achieve the effect of grain refinement, due to the limitation of molds, they are relatively problematic [23]. There are certain limitations in the industrial preparation of fine grains, meaning that it is difficult to adapt methods to the preparation of large-size metal plates or bulk materials [24]. Therefore, in this study, we intend to explore a simple and efficient method to refine the grains of cast pure copper via room-temperature compression.

Recrystallization is an important method to regulate grain sizes and is favored in practical manufacturing. Doherty et al. [25] clarified the concept of recrystallization. Driven by deformation energy storage, recrystallization occurs in a material, transforming small-angle grain boundaries into large-angle grain boundaries. Alongside the grain boundary migration process, a new crystal structure will be formed. Recrystallization nucleation and grain growth are two important processes of recrystallization [26]. The degree of deformation, annealing temperature, and holding time all affect the recrystallization rate of a material. The study of substructure dislocations during deformation and annealing is also an important direction in materials research [27].

Based on the above analysis, in this study, we intend to adopt the methods of compression at room temperature to induce a large deformation of pure copper through unidirectional compression followed by lamination compression. Then, deformed samples are recrystallized and annealed to explore the evolution of the microstructure and texture of pure copper during this process, aiming to provide insights into the grain refinement of advanced materials.

2. Materials and Methods

The material used was cast pure copper, which was commercially purchased. This material is also known as red copper; the name "pure copper" is used uniformly in this paper. The material grade in China is T2, corresponding to the Japanese standard grade C1100 and the American standard grade C11000. In terms of chemical composition, the copper content was Cu $\geq$ 99.90%. First, a pure copper ingot was cut into samples with a diameter of 8 mm and a height of 12 mm using a wire cutting machine; then, the material was compressed at room temperature with a large deformation degree on an MY-10 model oil press. Before the compression experiment, the upper and lower surfaces of the specimens in contact with the press were polished and flattened so as to reduce the experimental error as much as possible. The one-time compression could not reach more than 90% of the deformation degree; thus, the one-way compression amount was 75%. Then, two samples were stacked together to compress 75%, and the height of the sample was successfully

pressed from 12 mm to 0.75 mm. The total deformation degree was 93.75% (the deformation degree was equal to the percentage of the difference between the height of the sample after compression and the height of the sample before compression). The large deformation compression process (as shown in Figure 1) helps to overcome the problem of a "minimum compression thickness" caused by the elastic deformation of the press, thus allowing the material to obtain a large cumulative strain. Then, the compressed sample was placed in a high-temperature furnace with fixed carbon for annealing. The process parameters of the annealing are shown in Table 1.

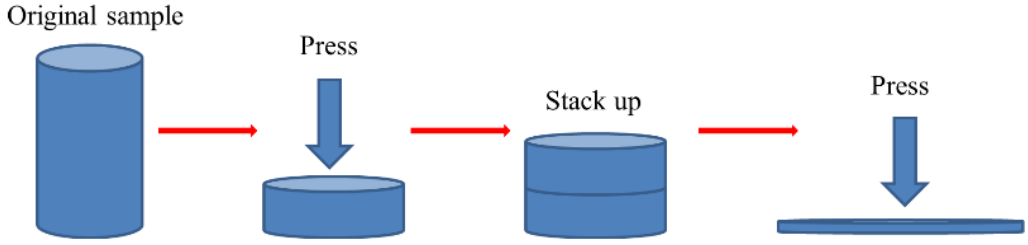

Figure 1. Large deformation compression process.

Table 1. Process parameters of the annealing test.

Material	Process Parameters
Pure copper	Annealing temperature: 350 °C
	Holding time: 5 min, 15 min, 30 min, 60 min

The hardness of the sample was tested via a microhardness tester. The testing load was 0.05 Kgf and the pressure holding time was 10 s. In order to reduce experimental error, seven different test points were marked near the central area of each sample, and the average arithmetic value after removing the maximum and minimum values during data processing was identified as the hardness value. In this experiment, a longitudinal section of the material was selected for microstructure analysis. First, the sample was sampled, inlaid, polished, and etched. The embedded sample was polished, using successive sandpaper grades from coarse to fine until the surface of the sample was smooth and without scratches. A water-soluble diamond grinding paste (type W1.0) was used for polishing. The etching agent was prepared by mixing 100 mL of alcohol, 15 mL of hydrochloric acid, and 5 g of ferric chloride, and the etching time was 15 s. The surface of the sample was polished via argon ion polishing technology with a strength of 5.5 KV. The longitudinal section of the compressed sample was selected for mechanical polishing, and an EBSD study was conducted via field emission scanning electron microscopy (FE-SEM) using a JEOL JSMIT 800 equipped with an Oxford C-nano EBSD detector at a step size of 0.16 μm and an accelerated voltage of 20 kV. Finally, the test data were analyzed using AZtecCrystal 2.1 data-processing software. In the above test, CA represents the compression direction, TD represents the conversion direction, and ND is the test direction, perpendicular to the test area. The microstructure of the etched sample was observed via SEM. The microstructure of the sample was imported into Nano Measurer 1.2 software to calculate the grain size distribution (the influence of the twin boundary was excluded). Five samples were analyzed for each project to ensure the accuracy of the results.

3. Results and Discussion

The hardness of pure copper before compression deformation is 72 HV. Figure 2 shows the hardness curve of pure copper after compression deformation and annealing at 350 °C under different holding times (neglecting anisotropy in hardness measurements). It can be seen in Figure 2 that the hardness of pure copper under large deformation is 110 HV, and when the annealing process is 350 °C × 5 min, the hardness is 73.24 HV. When the annealing process is 350 °C × 15 min, the hardness is 70.28 HV. When the annealing process is

350 °C × 30 min, the hardness is 68.00 HV. When the annealing process is 350 °C × 60 min, the hardness is 66.49 HV. It can be seen that for pure copper annealed at 350 °C, its hardness gradually decreases with an extension of the holding time. This is because the residual stress inside the metal is eliminated, static recrystallization occurs, and the hardness is thus reduced [28]. In general, the hardness and dislocation density within the material are closely related to the internal organization of the material. During the annealing process, recrystallization occurs, and the annealed dislocation density is significantly reduced, resulting in a significant decrease in hardness.

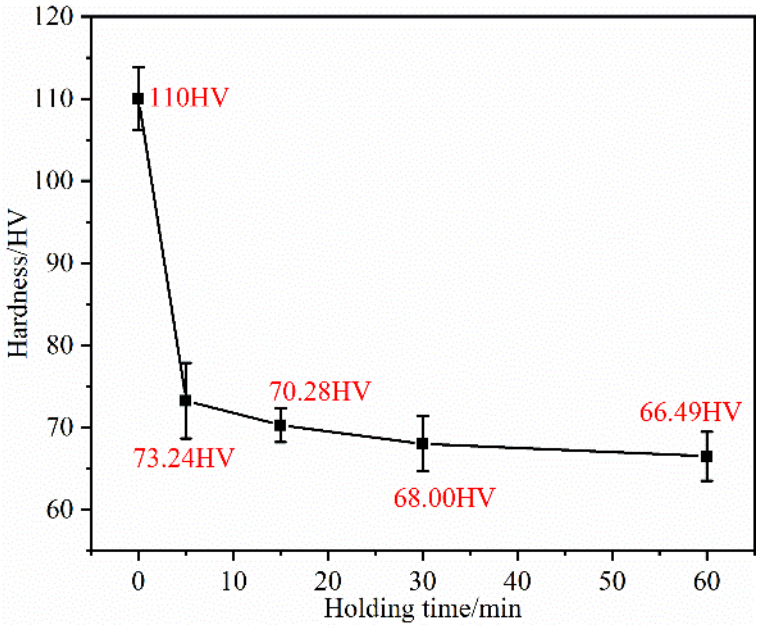

Figure 2. The hardness curve of pure copper after large compression deformation and annealing under different holding times.

The microstructure of pure copper before deformation is shown in Figure 3. It can be seen in Figure 3 that pure copper before deformation is composed of grains with sizes ranging from 50 μm to 200 μm, with irregular polygon structures and uneven grain sizes and an average grain size of 150 μm.

Figure 4 shows the microstructure of pure copper after cumulative deformation. As can be seen in Figure 4, the grains inside the material become flattened after compression, indicating that due to the excessive deformation of the material, the internal organization of the material is unstable, forming a shear band, where the direction of the shear band is about 20° from the direction of the metal flow. As shown in the mark in the figure, layered bands are generated in the internal area of the yellow box.

Annealing can enhance the properties of pure copper and, thus, reduce the defects in the structure of pure copper after compression deformation. During this process, non-distorted recrystallization grains and mobile high-angle grain boundaries easily form and static recrystallization occurs [29]. Figure 5 shows the microstructure of pure copper after cumulative compression deformation under different annealing conditions. In Figure 5a, we can see that the grains are compressed and flattening into equiaxed crystals, which indicates that at this time, the material is almost entirely internally recrystallized grains, as shown in Figure 5b–d. With the increase in the annealing time, the size and morphology of the grains did not significantly change, and there is no obvious deformation of the textile, which suggests that after the compression of the pure copper material and annealing at 350 °C for 5 min, almost complete recrystallization occurs. Increasing the annealing time did not further promote the recrystallization process.

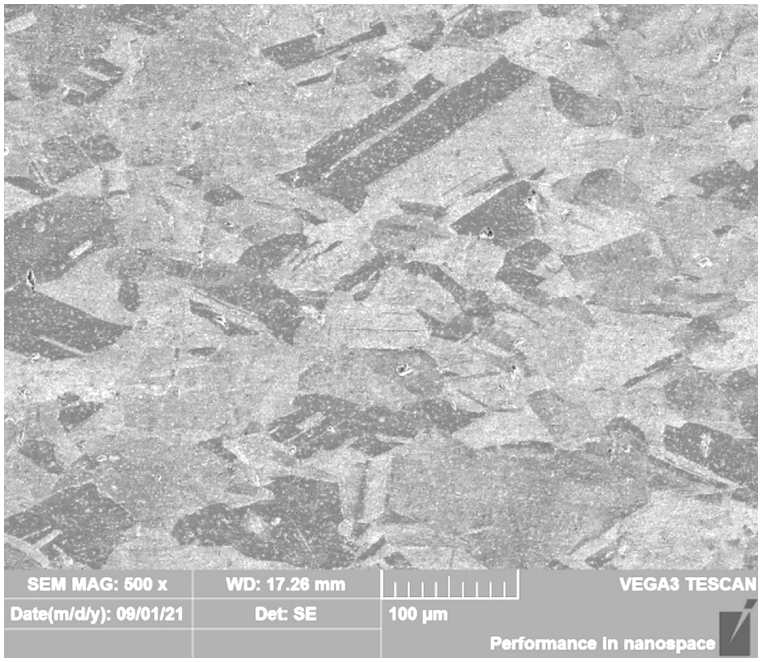

Figure 3. Microstructure of pure copper before deformation.

(**a**) (**b**)

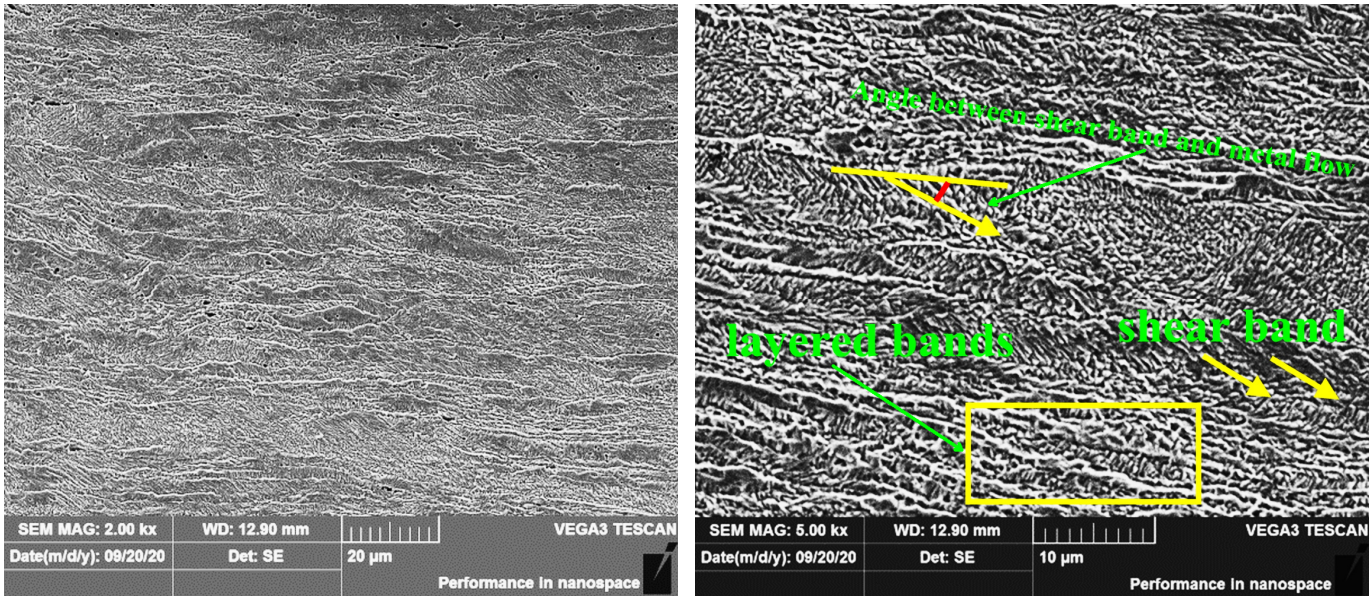

Figure 4. Microstructure of pure copper after cumulative deformation: (**a**) low magnification; (**b**) high magnification.

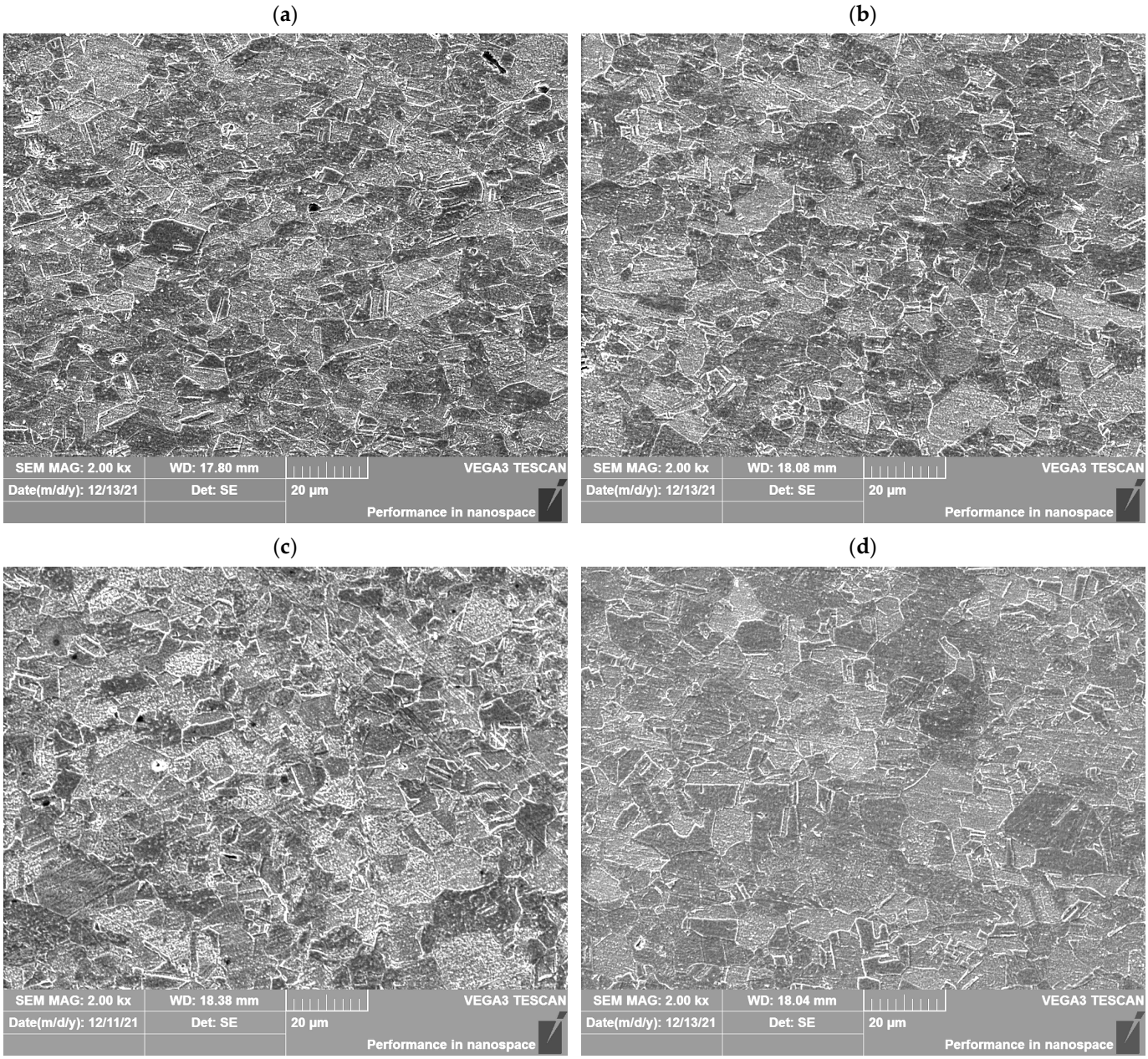

Figure 5. Microstructure of pure copper after cumulative compression under different annealing processes: (**a**) 350 °C × 5 min; (**b**) 350 °C × 15 min; (**c**) 350 °C × 30 min; (**d**) 350 °C × 60 min.

Figure 6 represents the grain size distribution of pure copper after cumulative compression and annealing under different annealing conditions. As can be seen in Figure 6, the average grain size is 6.15 µm with an annealing temperature of 350 °C and a holding time of 5 min. When the holding time is extended to 15 min, the grain size grows slightly, reaching an average grain size of 6.24 µm. When the holding time is 30 min, the average grain size is 6.39 µm. When the holding time is 60 min, the average grain size is 6.94 µm. However, the grain size changes marginally after annealing, indicating that for deformation degrees exceeding 90%, the annealing holding time has a small effect on grain refinement.

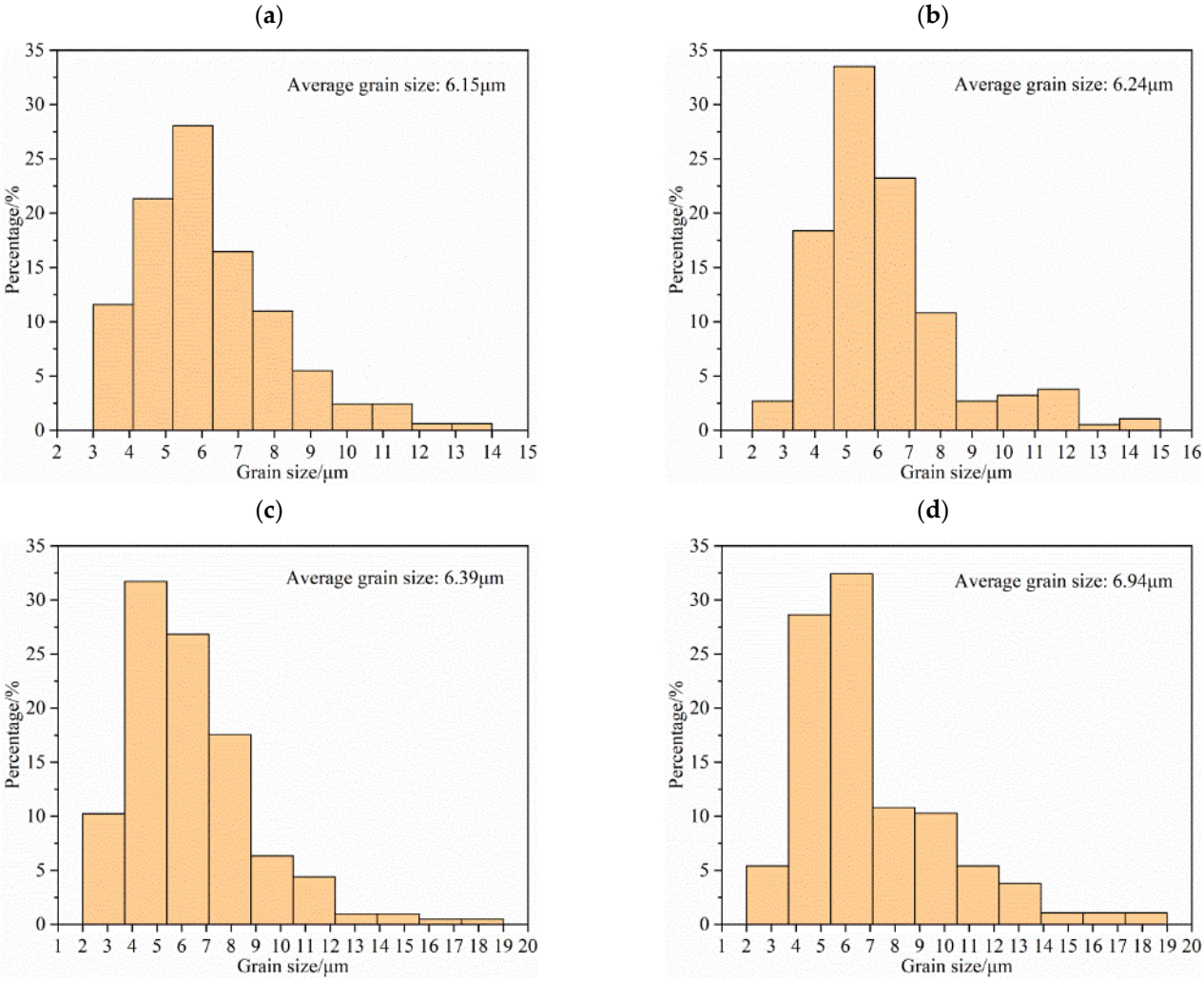

Figure 6. Grain size distribution of pure copper under different annealing conditions: (**a**) 350 °C × 5 min; (**b**) 350 °C × 15 min; (**c**) 350 °C × 30 min; (**d**) 350 °C × 60 min.

The EBSD method can be used to clearly analyze the relationships between deformation microstructure, annealing microstructure, and grain orientation. The specimens after compression annealing for 60 min and before annealing were selected for EBSD tests. Figure 7 illustrates images of the grain orientation of the pure copper samples before and after annealing and compression deformation. As can be seen in Figure 7a, basically all grains are obviously compressed into long strips. As can be seen in Figure 7c, the grains grow after annealing and become irregular polygons. Recrystallization is the most important stage in the annealing process of metals. It does not involve large-angle grain boundary migration; thus, the shape and size of the grain are the same as after deformation, maintaining a fibrous or flattened structure. In the recrystallization stage, the first step involves the production of a new core of distortion-free grains in regions with large distortion; then, the surrounding deformed matrix is gradually consumed until the structure is completely reorganized into new distortion-free, equiaxed grains (as shown in Figure 7c) [30,31]. Figure 7b,d show the grain size distribution of representative samples before and after annealing, and it can be seen that the grain size of the samples increased after annealing, and the percentage of 5–6 μm grains increased rapidly. This may be due to the fact that the defects and weaves generated under the cumulative deformation of pure copper during annealing are consumed by crystalline recrystallization, which provides energy for the secondary growth of the grains so that the grains can grow to a limited extent during annealing.

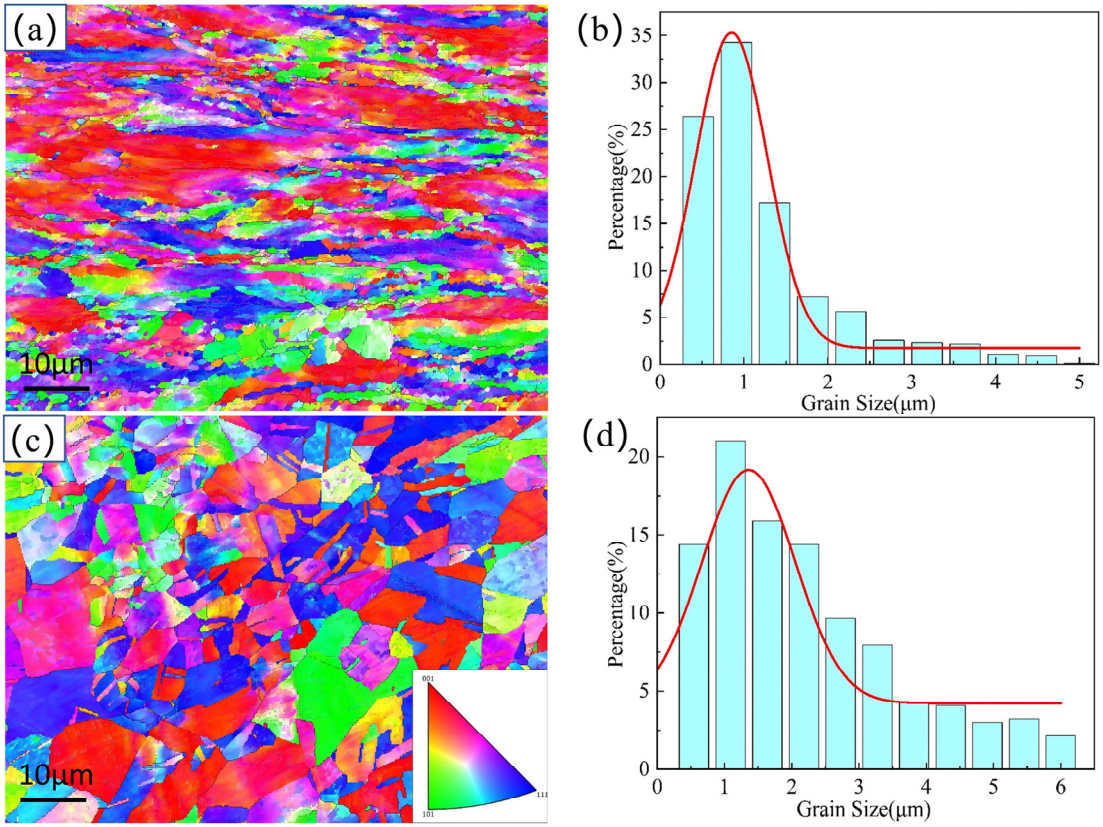

Figure 7. Grain orientation of pure copper specimens after compression deformation before and after annealing: (**a**,**b**) before annealing; (**c**,**d**) after annealing at 350 °C × 60 min.

Figure 8 shows the kernel-averaged misorientation (KAM) plots before and after annealing. The plots change from blue to green and finally to red, indicating a gradual increase in local orientation errors. The distribution of local orientation dislocations is related to the grain distribution, and orientation dislocations at grain boundaries are usually higher than those in the grains. This indicates that during compression, a large number of dislocations are present at the grain boundaries, the atoms at the grain boundaries are irregularly arranged, the lattice distortion is large, and dislocation stacking groups and plastic deformation are easily produced. In addition, the geometrically necessary dislocation (GND) density of the material before and after annealing was calculated. As shown in Figure 8, before annealing, a large number of dislocations are present at the grain boundaries due to compression, thus resulting in a larger ρGND. After annealing, the GND density decreases from $6.0 \times 10^{14}/m^2$ to $4.83 \times 10^{14}/m^2$, and dislocation consumption increases during the annealing process, thus resulting in a smaller ρGND density. This implies that static recrystallization occurs at the expense of dislocation consumption during annealing. This can also be reflected in the average grain orientation spread (GOS) map and the changes in low-angle grain boundaries (LAGBs) and high-angle grain boundaries (HAGBs). We mark the region with GOS < 3° as the recrystallized region, and it can be seen that the grain size at the grain boundaries after annealing becomes larger and more regular. The distribution of the dislocation density of the partially recrystallized grains inside the grains and the distribution of the recrystallized grains are highly correlated, and the GND density in the region where recrystallization occurs more sufficiently is obviously decreased. At the same time, the number of LAGBs inside the grain decreases, and the proportion of LAGBs is 68.7% and 31.3%, respectively (shown in Figure 9).

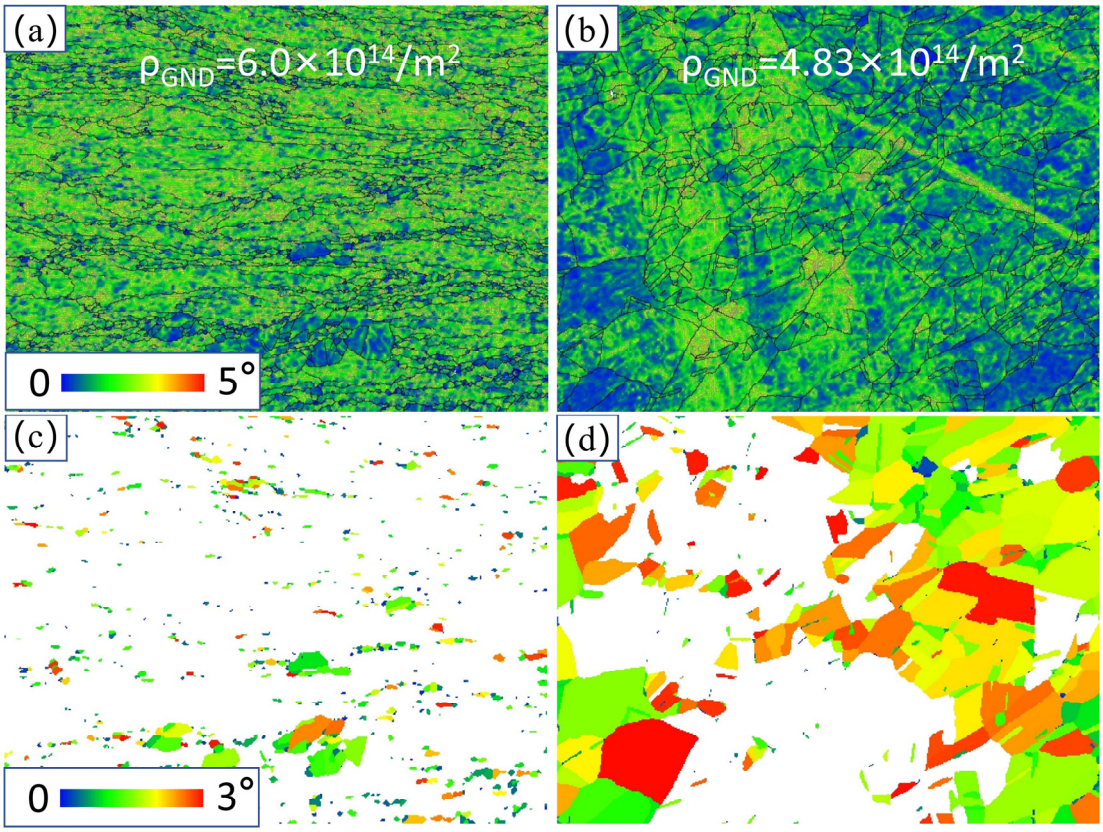

Figure 8. KAM and GOS plots of pure copper before and after annealing: (**a**,**c**) before annealing; (**b**,**d**) after annealing at 350 °C × 60 min.

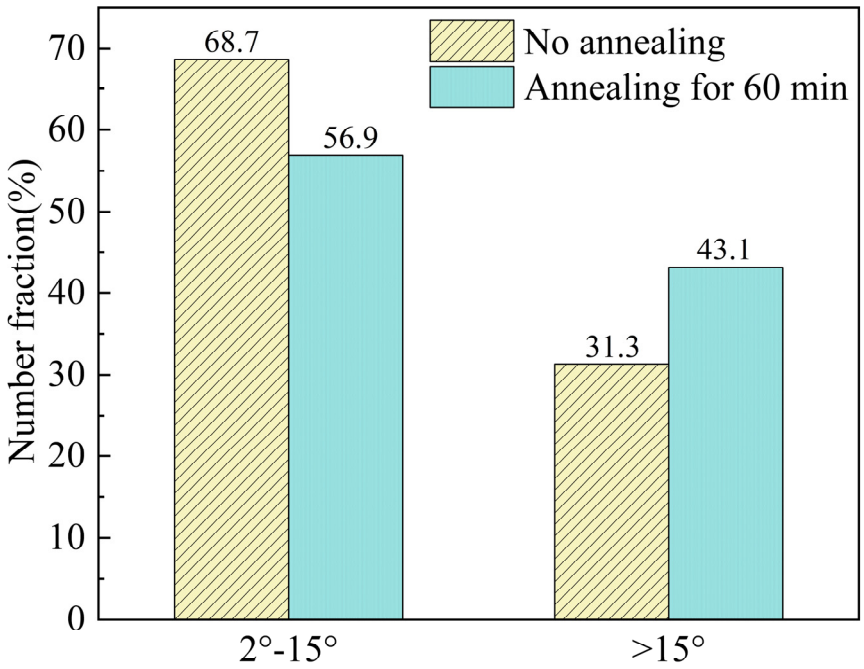

Figure 9. Changes in the LAGB and HAGB of pure copper specimens before and after annealing.

Figure 10 presents the pole figures of pure copper after compression deformation before and after annealing. Grains of pure copper are preferentially oriented before and after annealing, the poles after compression deformation are diffusively distributed, the

number of poles is small, and there are a few special aggregation points. By observing the pole figures in Figure 10, it can be seen that pure copper specimens at room temperature after compression deformation exhibit a clear grain orientation preference. The poles are symmetrically distributed in the pole plot, with the pole density levels ranging from 0 to 4.08, showing a generally regular distribution. The presence and high number of points with a pole density level close to 4.08 in the pole plots indicate that the grains are clearly oriented within the large, deformed specimens, and that a large number of weaves are present. However, in the annealed specimens, the number of points with a pole density level close to 3.85 is very small. This indicates that the grain orientation in annealed specimens is weak, and the number of textures is low. This is because the recrystallization annealing process eliminates part of the stress in the material and weakens the preferred orientation of the grain in the material.

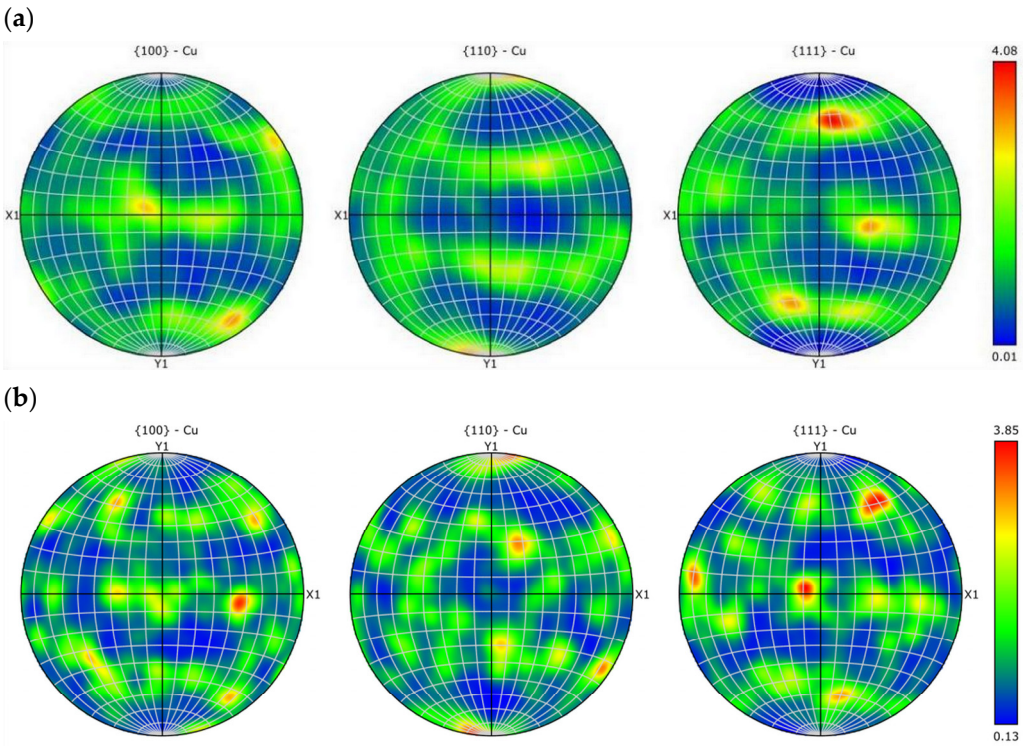

Figure 10. Pole figures of pure copper before and after annealing: (**a**) before annealing; (**b**) after annealing at 350 °C × 60 min.

Different orientations of the grains can reflect different deformation degrees, and the texture types of different pure copper grains after compression deformation at room temperature exhibit differences; that is, various preferred orientations are produced. As pure copper is a face-centered cubic metal and a low-level fault energy metal, plastic deformation depends on the sliding action. When pure copper is compressed at room temperature, the external forces acting on grains with different orientations also vary, and even different positions of the material will affect the external forces on the grains; therefore, not all grains undergo plastic deformation at the same time. Grains at the center preferentially deform, while grains at the edges do not deform permanently. The grain slip system at different orientations is different and the slip directions in the same slip system are also different. In the process of compression deformation at room temperature, the internal grains of the material coordinate with each other to ensure the continuity of plastic deformation, with different grains showing a greater inclination to deform in powerful slip systems [32,33].

Figure 11 shows the inverse pole figure of the compression direction (CA axis) of the pure copper sample before and after annealing. In Figure 11a, we can see that when pure

copper is compressed at room temperature, there is a strong <111> texture in the sample. In Figure 11b, we can see that after compression and annealing at 350 °C for five minutes, the compressed specimen still has the preferred orientation, with the percentage of <111> orientation increasing dramatically compared to the unannealed specimen, which indicates that the annealed fabrics are not consistent with the original fabrics and that a larger number of fiber fabrics with <001> and <111> orientations are simultaneously present within the annealed specimen. The main reason for this phenomenon is that when pure copper is compressed, the material undergoes internal fabric deformation. Most grains exhibit a close grain orientation (manifested as <001>). At this point, grain growth is restricted, and some of the deformed organization exhibits a special relationship between the phases of nucleus recrystallization. The grain boundaries exhibit a very high migration velocity, leading to preferential growth. Gradually, they consume the surrounding deformed matrix and come into contact with each other, thus forming the deformation with the fabric contact and forming a recrystallized structure (<111>) with a different orientation than the deformed structure. In this process, the recrystallized weave does not completely replace the deformed weave, but it weakens the strength of the deformed weave to a certain extent (as shown in Figure 11, the strength of the <001> orientation before and after annealing is reduced from 2.15 to 1.94), resulting in the existence of two types of strong weaves within the material at this stage, i.e., compression-generated deformed weaves (<001>) and recrystallized weaves produced via annealing (<111>).

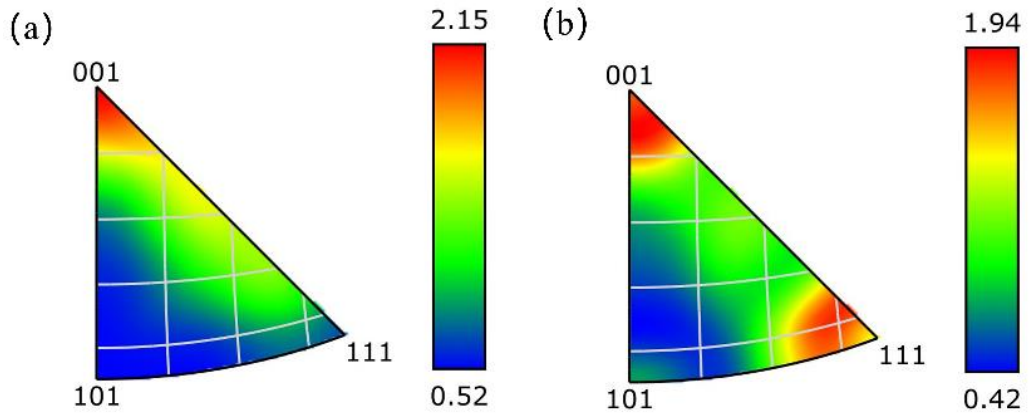

Figure 11. Antipodal plots of pure copper specimens in the direction of CA axis before and after annealing and compression deformation: (**a**) before annealing; (**b**) after annealing at 350 °C × 60 min.

4. Conclusions

Through the compression deformation and annealing of cast pure copper, the following important conclusions can be drawn:

(1) When the compression deformation was 93.75%, the microhardness of pure copper rose from 76 HV to 110 HV. After annealing at 350 °C, with an increase in the annealing time, the hardness decreased, and the pure copper grain was refined from the original 150 μm to 6.15 μm;

(2) An increase in the annealing time did not promote recrystallization, while the effect on grain refinement was weakened;

(3) The GND density decreased from $6.0 \times 10^{14}/m^2$ to $4.83 \times 10^{14}/m^2$ after annealing, which implies that static recrystallization occurred at the cost of dislocation consumption during the annealing process;

(4) The compressive deformation of pure copper produced a strong deformation weave (<001> orientation), and a portion of the deformation weave within the material was transformed into a recrystallization weave (<111> orientation) after the annealing process.

Author Contributions: Conceptualization, methodology, investigation, and data curation, X.L.; writing—original draft, X.L. and Q.Z.; software, Q.Z. and W.L.; conceptualization and writing—review and editing, W.L.; methodology, study design, and writing—review and editing, F.L., J.L. and S.G. All authors have read and agreed to the published version of the manuscript.

Funding: This work is supported by the Scientific and Technological Research Project of Henan Province (No. 232102230059), the Henan University of Science and Technology 2021 Young Backbone Teacher Training Program (No. 13450023), and the Longmen Laboratory frontier exploration project (No. LMQYTSKT001).

Institutional Review Board Statement: Not applicable.

Informed Consent Statement: Not applicable.

Data Availability Statement: Data are contained within the article.

Acknowledgments: We thank the support of the Provincial and Ministerial Collaborative Innovation Center of Non-ferrous Metal New Materials and Advanced Processing Technology.

Conflicts of Interest: Fengjun Li was employed by the First Tractor Company Limited, Jianjun Liang and Shimin Gu were employed by the Nanyang North Hongyu Electromechanical Manufacturing Company Limited. The remaining authors declare that the research was conducted in the absence of any commercial or financial relationships that could be construed as a potential conflict of interest. The funders had no role in the design of the study; in the collection, analyses, or interpretation of data; in the writing of the manuscript; or in the decision to publish the results.

References

1. Zhang, D.; Lu, P.; He, X.; Gao, Y. Abrasive Wear and Physical Properties of In-Situ Nano-TiC_x Reinforced Cu-Cr-Zr Composites. *Coatings* **2023**, *13*, 1263. [CrossRef]
2. Wang, Y.; Xu, L.; Li, X. Study on Microstructure and Mechanical Properties Modification of Cu-Ti_3AlC_2 Composites by Ni Element. *Coatings* **2023**, *13*, 13081414. [CrossRef]
3. Ji, B.; Zhang, H.; Cao, J.; Zhang, Q. Evaluation of the Thickness of Each Layer of Cu/Al Laminate Using Laser Ultrasonic. *Coatings* **2023**, *13*, 645. [CrossRef]
4. Song, B.; Yu, T.; Jiang, X.; Xi, W.; Lin, X. Effect of W content on the microstructure and properties of Cu-Fe alloy. *J. Mater. Res. Technol.* **2020**, *9*, 193–205. [CrossRef]
5. Zhu, J.; Liu, S.; Liu, Y.; Lin, N.; Yang, S.; Deng, C.; Liu, Q. Deformation and annealing behavior in the 'interaction zone' of cold-rolled tantalum sheets. *Vacuum* **2019**, *164*, 105–113. [CrossRef]
6. Deng, C.; Liu, S.; Ji, J.; Hao, X.; Zhang, Z.; Liu, Q. Texture evolution of high purity tantalum under different rolling paths. *J. Mater. Process. Technol.* **2014**, *214*, 462–469. [CrossRef]
7. Liu, Q. Research progress on plastic deformation mechanism of Mg alloys. *Acta Metall. Sin.* **2010**, *46*, 1458–1472. [CrossRef]
8. Chan, W.; Fu, M.; Yang, B. Study of size effect in micro-extrusion process of pure copper. *Mater. Des.* **2011**, *32*, 3772–3782. [CrossRef]
9. Pfetzing-Micklich, J.; Brinckmann, S.; Dey, S.R.; Otto, F.; Hartmaier, A.; Eggeler, G. Micro-shear deformation of pure copper. *Mater. Und Werkst.* **2011**, *42*, 219–223. [CrossRef]
10. Yannick, C.; Cyril, L.; Sandrine, G.; Langlois, P.; Bonnentien, J.-L.; Hÿtch, M.J. Near-perfect elastoplasticity in pure nanocrystalline copper. *Science* **2003**, *300*, 310–311.
11. Sakharov, N.V.; Chuvil'deev, V.N. Model of Primary Recrystallization in Pure Copper. *Phys. Met. Metallogr.* **2021**, *122*, 673–680. [CrossRef]
12. Konkova, T.; Mironov, S.; Korznikov, A.; Semiatin, S. Microstructural response of pure copper to cryogenic rolling. *Acta Mater.* **2010**, *58*, 5262–5273. [CrossRef]
13. Song, K.; Han, S.; Kim, W. Effects of Strain Rate in Cold-Rolled Pure Copper Produced by Different Rolling Processes. *Mater. Sci. Forum* **2011**, *695*, 307–311. [CrossRef]
14. Xu, H.; Hu, W.; Kang, C.; Li, W.; Sha, X. Microstructure evolution during annealing at different temperatures and hot deformation behavior of lean duplex stainless steel 2101. *Steel Res. Int.* **2021**, *92*, 2000264. [CrossRef]
15. Zhao, Y.; Horita, Z.; Langdon, T.; Zhu, Y. Evolution of defect structures during cold rolling of ultrafine-grained Cu and Cu-Zn alloys: Influence of stacking fault energy. *Mater. Sci. Eng. A* **2008**, *474*, 342–347. [CrossRef]
16. Chen, Q.; Shu, D.Y.; Lin, J.; Wu, Y.; Xia, X.; Huang, S.; Zhao, Z.; Mishin, O.; Wu, G. Evolution of microstructure and texture in copper during repetitive extrusion-upsetting and subsequent annealing. *J. Mater. Sci. Technol.* **2017**, *33*, 690–697. [CrossRef]
17. Lee, H.; Im, Y. Cellular Automata Modeling of Grain Coarsening and Refinement during the Dynamic Recrystallization of Pure Copper. *Mater. Trans.* **2010**, *51*, 1614–1620. [CrossRef]
18. Gao, Y.; Ding, Y.; Chen, J.; Xu, J.; Ma, Y.; Zhang, D. Evolution of Microstructure and Texture During Cold Deformation of Hot-Extruded GH3625 Alloy. *Acta Met. Sin.* **2019**, *55*, 547–554.

19. Wu, Z.; Jing, C.; Feng, Y.; Li, Z.; Lin, T.; Zhao, J. Effects of different annealing time on microstructure and mechanical properties of lightweight Al-containing medium-Mn steel. *Ironmak. Steelmak.* **2023**, 1–11. [CrossRef]
20. Ohyama, H.; Akiyama, M. Development and Evaluation of Environmentally Friendly Lubricantfor Cold Metal Working. *J. Jpn. Soc. Technol. Plast.* **2011**, *52*, 474–479.
21. Singh, V. Effects of prior cold working on low cycle fatigue behavior of stainless steels, titanium alloy timetal 834 and superalloy IN 718: A review. *Trans. Indian Inst. Met.* **2010**, *63*, 167–172. [CrossRef]
22. Wang, S.; Wu, Z.H.; Xie, M.Y.; Si, D.H.; Li, L.Y.; Chen, C.; Zhang, Z.; Wu, Y.C. The effect of tungsten content on the rolling texture and microstructure of Ta-W alloys. *Mater. Charact.* **2020**, *159*, 110067. [CrossRef]
23. Balasundar, I.; Ravi, K.R.; Raghu, T. Strain softening in oxygen free high conductivity (OFHC) copper subjected to repetitive upsetting-extrusion (RUE) process. *Mater. Sci. Eng. A* **2013**, *583*, 114–122. [CrossRef]
24. Pardis, N.; Chen, C.; Ebrahimi, R.; Toth, L.S.; Gu, C.F.; Beausir, B.; Kommel, L. Microstructure, texture and mechanical properties of cyclic expansion-extrusion deformed pure copper. *Mater. Sci. Eng. A* **2015**, *628*, 423–432. [CrossRef]
25. Yan, X.; Wu, Y.; Zhang, M.; Liu, S.; Sun, L.; Feng, Y. Microstructure Evolution and Mechanical Properties of Ferrite–Austenite Duplex Fe-Mn-Al-(Cu)-C Steel under Different Annealing Temperatures. *Materials* **2022**, *15*, 8271. [CrossRef] [PubMed]
26. Li, W.; Liu, P.; Ma, F.; Liu, X.K.; Chen, X.H.; Zhang, Y. Effects of Aging and Cold Deformation on Microstructure and Properties for Cu-Ni-Si Alloy. *Rare Met.* **2011**, *35*, 330–335.
27. Pogrebnjak, A.D.; Bagdasaryan, A.A.; Horodek, P.; Tarelnyk, V.; Buranich, V.V.; Amekura, H.; Okubo, N.; Ishikawa, N.; Beresnev, V.M. Positron annihilation studies of defect structure of (TiZrHfNbV)N nitride coatings under Xe14+200 MeV ion irradiation. *Mater. Lett.* **2021**, *303*, 130548. [CrossRef]
28. Gao, X.; Wu, H.; Liu, M.; Zhang, Y.-X. Effect of annealing time on grain boundary characteristics of C71500 cupronickel alloy tubes with different deformation. *Mater. Charact.* **2020**, *169*, 110603. [CrossRef]
29. Ding, C.; Xu, J.; Shan, D.; Guo, B.; Langdon, T.G. The thermal instability mechanism and annealed deformation behavior of Cu/Nb nanolaminate composites. *J. Mater. Sci. Technol.* **2023**, *157*, 163–173. [CrossRef]
30. Li, H.; Huang, Y.; Liu, Y. Dynamic recrystallization mechanisms of as-forged Al–Zn–Mg-(Cu) aluminum alloy during hot comp. ression deformation. *Mater. Sci. Eng. A* **2023**, *878*, 145236. [CrossRef]
31. Chandra, S.; Alankar, A.; Kumar, N.N.; Samal, M.K.; Chavan, V.M. An atomistic analysis of the effect of grain boundary and the associated deformation mechanisms during plain strain compression of a Cu bicrystal. *Comput. Mater. Sci.* **2022**, *202*, 110953. [CrossRef]
32. Shahmir, H.; Nili-Ahmadabadi, M.; Mohammadi, M.; Huang, Y.; Andrzejczuk, M.; Lewandowska, M.; Langdon, T.G. Effect of Cu on amorphization of a TiNi alloy during HPT and shape memory effect after post-deformation annealing. *Adv. Eng. Mater.* **2020**, *22*, 1900387. [CrossRef]
33. Feng, X.; Lin, Z.; Xin, K.; Pang, W. The deformation mechanisms and mechanical properties of Cu/Fe multilayer during compression process. *J. Mater. Res.* **2021**, *36*, 3203–3213. [CrossRef]